J. Nanoanalysis., 6(1): 48-56, Winter 2019

ORIGINAL RESEARCH PAPER

Electrodeposition of anionic, cationic and nonionic surfactants and gold nanoparticles onto glassy carbon electrode for catechol detection

Maryam Nazari[1,3], Soheila Kashanian[2,3,*], Rezvan Mohammadi[1]

[1] Faculty of Chemistry, Razi University, Kermanshah, Islamic Republic of Iran

[2]Faculty of Chemistry, Sensor and Biosensor Research Center (SBRC) and Nanoscience and Nanotechnology Research Center (NNRC), Razi University, Kermanshah, Islamic Republic of Iran

[3]Nano Drug Delivery Research Center, Faculty of Pharmacy, Kermanshah University of Medical Sciences, Kermanshah, Iran

Received: 2018-10-01 Accepted: 2018-11-28 Published: 2019-02-01

ABSTRACT

Three surfactants were selected to modify glassy carbon electrode including sodium dodecylbenzenesulfonate, Tween 80 and cetyltrimethylammonium bromide. The obtained nano-Au/surfactant/GCEs were characterized with scanning electron microscopy and electrochemical techniques. Electrochemical behavior of catechol at the nano-Au/surfactant/GCE was thoroughly investigated for modified electrodes. Compared to the unmodified electrode, the peak current obviously increased and the oxidation and reduction peaks potential shifted to the negative and positive potential area, respectively, meaning the peak potential separation is reduced. These changes indicated that the composite nanoparticles possess good electrocatalytic performance on the electrochemical reaction of catechol. The experimental results revealed that the nanoparticle modified electrodes have good performances for catechol sensing, which including convenient fabrication, low detection limits and wide linear ranges. These merits of this sensing system provide high potential to apply in environmental monitoring. In addition, kinetic parameters of catechol redox reaction were determined and the number of electrons was obtained two for the three modified electrodes.

Keywords: *Catechol; Cetyltrimethylammonium Bromide; Gold Nanoparticle; Sodium Dodecylbenzene Sulfonate; Tween 80*

How to cite this article

Nazari M, Kashanian S, Mohammadi R. Electrodeposition of anionic, cationic and nonionic surfactants and gold nanoparticles onto glassy carbon electrode for catechol detection. J. Nanoanalysis., 2019; 6(1): 48-56.

DOI: 10.22034/jna.2019.664401

INTRODUCTION

A large variety of phenolic compounds are widely used in the manufacture of products, including coal conversion, petroleum refining, pharmaceuticals, production of dyes, pesticides, resins, and plastics and thus readily release into the ground and surface water [1-3]. The identification and quantification of these compounds are important for environmental monitoring because many of them are toxic contaminants in medical, food and environmental matrices and have harmful effects on plants, animals and human health [4-6]. The maximum amount of phenols in wastewater allowed by the European Community is lower than 1 ppm [7]. Many analytical methods are available for the determination of them, such as spectrophotometry, chromatography, and capillary electrophoresis. However, these methods are time-consuming and the instrumentations are expensive [8,9]. Sensors can provide ideal sensing systems

* Corresponding Author Email: *kashanian_s@yahoo.com*

to monitor the effects of phenolic compounds on the environment, due to their fast response, high selectivity, cost-effectiveness, simplicity of operation, and manufacturing. Electrochemical techniques such as voltammetry are particularly attractive since they are fast, sensitive, and amenable to portability and have low instrumental cost [9-12]. Using nanoparticles (NPs) in the fabrication of electrochemical sensors enhances selectivity and sensitivity. Gold nanoparticles (AuNPs) have good conductivity and strong adsorption ability. Furthermore, AuNPs can promote the electron transfer. AuNPs show mimic enzyme activity, especially for sensing of phenolic compound. Under similar conditions, metal nanomaterials like Ag, Cu, Pt, and Pd which were used, did not display significant oxidase mimic activity. AuNPs could be used for redox proteins or enzymes immobilization with high stability by keeping their bioactivity for development of biosensors [13,14]. In addition, AuNPs can conjugated to proteins, enzymes and other biomolecules easily [15]. The choice of a good stabilizer is essential, because it accelerates the rate of metal particle formation and markedly reduces the rate of metal deposition, and also protects the metal NPs from agglomeration [16]. Khan M.N. *et al.* reported that $AuCl_4^-$ species aggregated in an unsymmetrical manner due to the morphology of gold nanostructures, which can cause the formation of beautiful nano-flower like gold [17]. Surfactants have been commonly utilized as a good stabilizer in the synthesis of NP [18]. They can be adsorbed on the electrode surface and modify the properties of electrode/solution, and enhance stability, and detection sensitivity, as reported in the literature [19-23]. They play a crucial role in the area of electrodes with modified surface, not only in solubilizing organic compounds, but also by providing specific orientation of the molecules at the electrode interface [24]. Cetyl trimethyl ammonium bromide (CTAB) can change the mechanism of Cu dissolution in acidic media by forming film on the electrode surface [25].

Using surfactants for electrode modification has got great interest. For example, Yang Y. J., *et al.*, used GCE modified with electropolymerized CTAB for detection of analytes including tryptophan, theophylline, uric acid, and dopamine [26]. Patnaik P., *et al.* investigated the influence of Tween 80 on Cobalt electrochemical deposition [27]. Zhang J., *et al.*, used SDBS modified graphite paste electrode for dopamine selective detection [28].

Valezi, C.F., *et al.* have developed an analytical procedure using multi-walled carbon nanotubes modified paste electrode in the presence of cationic surfactant CTAB. They found that the positive charges of CTAB can influence on the electrochemical response of analyte at electrode surface [29]. Peng, J. and Z.-N. Gao have studied the electrochemical behavior of catechol and hydroquinone in aqueous cetylpyridinium bromide (CPB) and SDBS solutions using cyclic voltammetry (CV). They understood that CPB can promote the electrochemical oxidation reactions of catechol and hydroquinone, and SDBS can inhibit these electrochemical oxidation reactions [30]. Zhao Y., *et al.* reported that Tween 80, between Tween series of nonionic surfactants could be adsorbed on AuNPs, making the NPs most stably dispersed in aqueous solutions [31].

In this study, three different surfactants, including CTAB, Tween 80 and SDBS, were used for electrodeposition of AuNPs onto the electrode surface and utilized to investigate catechol electrochemical behavior. In the older works, the behavior of catechol in the presence of surfactants was investigated, but the electrochemical behavior of catechol was studied after electrodeposition of AuNPs and three surfactants on the electrode surface. The modification of the electrodes was verified by different techniques.

EXPERIMENTAL

Materials and instrumentations

CV and linear sweep voltammetry (LSV) were performed with a Sama 500 electroanalyzer system in a conventional three-electrode cell. Glassy carbon electrode was used as working electrode. An Ag/AgCl electrode (saturated KCl) and a Pt rod were used as reference and counter electrodes, respectively.

Scanning Electron Microscopy (SEM) (MIRA3 TESCAN) was used to characterize the electrode surface morphology. Electrochemical Impedance Spectroscopy (EIS) measurements were performed on Autolab (Eco Chemie BV, Netherlands) in 0.1 M KCl solution containing 5.0 mM $K_4[Fe(CN)_6]$/$K_3[Fe(CN)_6]$. Catechol was purchased from Merck, and their 0.01 M stock solutions were prepared in water. $HAuCl_4$ was brought from Pubchem. SDBS and Tween 80 were purchased from Merck and CTAB was purchased from Sigma. All other chemicals were of analytical grade and all of the solutions were prepared with deionized water.

Preparation of nano-Au/surfactant/GCE

A GCE was polished with fine emery paper and alumina slurries followed by rinsing thoroughly with ultrapure water and then allowed to dry at room temperature. Subsequently, in a 0.1 M KNO_3 solution containing 100 µM $HAuCl_4$ and 500 µM surfactant (SDBS, Tween 80, CTAB) the cleaned electrode was electrochemically treated under the constant potential of -0.4 V (vs. Ag/AgCl) for 300 s to obtain the nano-Au/surfactant/GCE. The modified electrode was then taken out of the cell and thoroughly rinsed with ultrapure water to remove the physically absorbed $HAuCl_4$ and surfactants. After that, it was scanned in a phosphate buffer (PB) solution to obtain a steady state with CV. GCE modified with surfactant-AuNPs was prepared using electrodeposition at constant potential of -0.40 V during 300 s and characterized with SEM and electrochemical techniques. Also, CV and EIS was employed to study the electrochemical behavior of catechol at the modified electrode.

RESULTS AND DISCUSSION

Electrode surface morphology and surfactant-capped

Fig. 1 shows the SEM top views of three different electrodes. As shown in the Fig. 1 A, B, C NPs were distributed on the electrode surface. In the case of nano-Au/Tween 80/GCE and nano-Au/SDBS/GCE, it is noticed that AuNPs are formed under the Au/surfactant capping agent on the electrode surface due to the Au peak observation in PB solution using CV technique (Fig. 1D). The SEM images show different surface morphologies. It is noticed that the vacant spaces for Au/CTAB are more decreased comparable to Au/SDBS and Au/Tween 80 according to Fig. 1 which indicate electrodeposition of Au/CTAB as an almost uniform film. This is a good evidence to confirm the electrochemical formation of three kind of surfactant-AuNPs on the electrode surface simply by one-step process. The CTAB molecules on the surface of AuNPs are in the bilayer structure [31] and it can occur after applying the potential in this experiment. Also, it should be noted that the applied potential is negative and therefore positive CTAB molecules can be adsorbed on the electrode surface due to the electrostatic interactions between them.

Table 1 shows the EDS analysis for nano-Au/Tween 80/GCE and nano-Au/SDBS/GCE. As can be seen gold is appeared to both of them. The presence of "S" for nano-Au/SDBS/GCE is related to sulfonate group of SDBS.

Electrochemical impedance characterization

EIS was used to investigate the impedance changes of the modified electrode surface. The diameter of the semicircle usually equals to the electron-transfer resistance (R_{et}), which controls the electron transfer kinetics of the redox probe ($K_3Fe(CN)_6/K_4Fe(CN)_6$) at the electrode interface. Fig. 2A illustrates the typical results of EIS of modified electrodes. The circuit of GCE, Au/CTAB/GCE and nano-Au/Tween 80/GCE was

Table 1. EDC analysis data

Element	nano-Au/ SDBS/GCE [wt.-%]	nano-Au/Tween 80/GCE [wt.-%]
Carbon	78.80	69.34
Nitrogen	0.05	0.06
Oxygen	14.40	24.79
Sodium	0.11	-
Aluminum	1.90	4.06
Sulfur	0.38	-
Potassium	0.80	0.13
Gold	3.54	1.62
Total	100	100

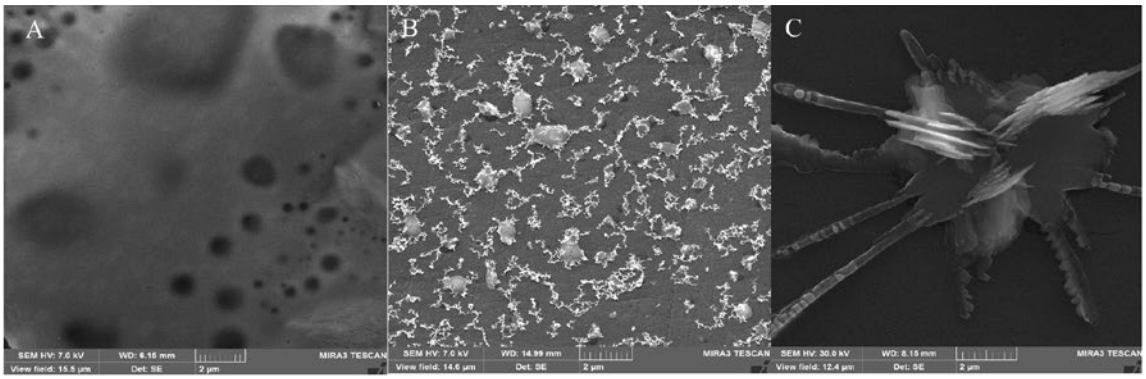

Fig. 1. SEM images of (A) nano-Au/CTAB/GCE, (B) nano-Au/Tween 80/GCE and (C) nano-Au/SDBS/GCE.

obtained [RQ(RW)] and the circuit of nano-Au/ SDBS/GCE is different from the others, which is obtained [RQ(RQ)]. Obviously, the bare GCE exhibited a semicircle portion with a diameter value of R_{et} that was estimated to be 1.85 kΩ. While the Nyquist plots of the nano-Au/SDBS/GCE, nano-Au/CTAB/GCE and nano-Au/Tween 80/ GCE showed semicircles with the value of R_{et} to be about 3.13 kΩ, 89.4 Ω and 2.50 kΩ, respectively. The relatively small R_{et} values found in the nano-Au/CTAB/GCE indicate that Au/CTAB composite promote the electron-transfer of electrochemical probes which confirming the CTAB capping agent on the electrode surface due to the easily oxidation and reduction of negative charge redox probe. By comparing the R_{et} values of three modified electrodes, a larger electron-transfer resistance was obtained at the nano-Au/SDBS/GCE. From EIS obtained data, the electron transfer mechanism in surface of nano-Au/CTAB/GCE is under diffusion control while in the other modified electrodes it is under kinetic control.

Effect of pH

The effect of pH on the current responses of catechol oxidation has been shown in Fig. 3A. In general, the current signal increases with rising the pH of the solution (up to pH 6), and then the current declines for the pH higher than 6 for two modified electrodes (nano-Au/CTAB/GCE (curve

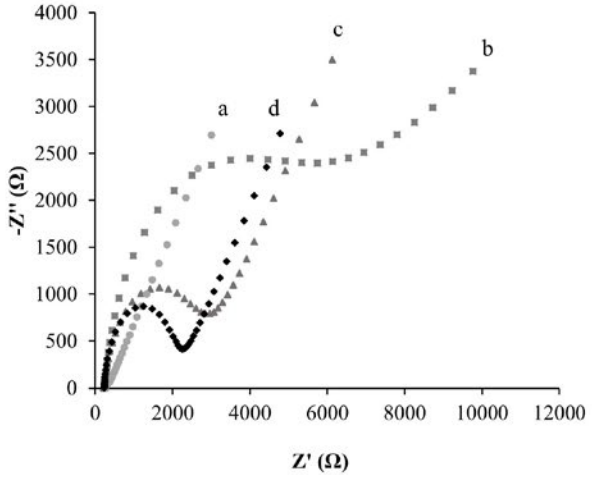

Fig. 2. (A) EIS of the nano-Au/CTAB/GCE (a), nano-Au/Tween 80/GCE (b), nano-Au/ SDBS/GCE (c) and the bare GCE (d) in KCl (0.1 M) solution containing $K_3Fe(CN)_6/K_4Fe(CN)_6$ (5.0 mM).

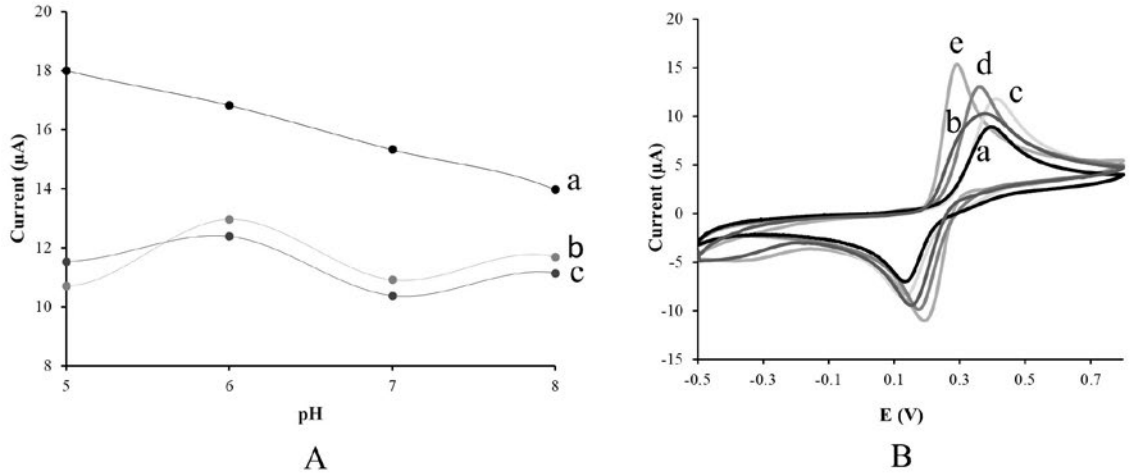

Fig. 3. (A) The effect of pH on the current responses of catechol oxidation for nano-Au/CTAB/GCE (a), nano-Au/Tween 80/GCE (b) and nano-Au/ SDBS/GCE (c). (B) CV voltammograms for GCE (a), nano-Au/GCE (b) nano-Au/CTAB/GCE (c), nano-Au/Tween 80/ GCE (d), nano-Au/ SDBS/GCE (e) in PB (0.1 M, pH 6) containing 1.0 mM catechol. Scan rate: 100 mV/s.

a), nano-Au/Tween 80/GCE (curve b)) (Fig. 3A). The peak currents of catechol gradually decreased with increasing the pH values from 5.0 to 8.0, resulting from the shortage of protons at higher pH values for nano-Au/SDBS/GCE. It has been well-known that the two isomers are protic aromatic molecules, which easily undergo deprotonation and turn to anions at high pH. Thus, as the pH increased to higher values, catechol was easily turned into anions, resulting in the electrostatic repulsion between catechol and the modified electrodes. Moreover, the solution experienced a shortage of protons, resulting in decrease of peak current [32]. The currents increased at lower pH values and decreased at higher pH values; lower pH values might lead to release of hydrogen, which might affect the nano-Au/SDBS for catechol adsorption and higher pH values turn catechol into anions and catechol anions could hardly participate in electrochemical reaction. To compare these electrodes, the experiments were done on the same pH (pH 6).

Electrochemical behavior of catechol

The detection of catechol is an important application field for the three modified electrodes. Catechol is used herein as a model of phenolic substrate to be detected. The electrochemical behavior of catechol was examined using CV at modifying electrodes (Fig. 3C). The redox properties of a compound are readily characterized by CV. Catechol gave two redox peak potentials for each material that we coated on the surface of the GCE, one anodic peak potential (E_p^a) related to the oxidation of catechol to o-quinone and one cathodic peak potential (E_p^c) related to the reduction of o-quinone to catechol. Fig. 3C shows the current–potential curves for GCE, nano-Au/GCE, nano-Au/CTAB/GCE, nano-Au/Tween 80/GCE, and nano-Au/SDBS/GCE electrodes. Table 3 indicates the data about E_p^a and E_p^c and also i_p^a and i_p^c for GCE, nano-Au/CTAB/GCE, nano-Au/Tween 80/GCE, and nano-Au/SDBS/GCE electrodes. The oxidation and reduction peak potentials showed negative and positive shifts respectively in the presence of surfactants indicating that the electron transfer between the electrode and bulk solution of catechol was facilitated. In comparison to CV peaks of catechol at modified and bare GCE, modified electrodes shown higher current peaks. Comparing the anodic currents of the electrodes indicated in Table 3, the nano-Au/SDBS/GCE has the highest anodic and cathodic currents. Decreasing the peak potential separation of modified electrodes indicates an increase in reversibility and facilitates the transport of electrons for catechol reduction and oxidation. As the nano-Au/SDBS/GCE has the highest current, and lowest difference between

Table 2. Anodic and cathodic currents and potentials in PB (0.1 M, pH 6.0) containing 1.0 mM catechol for GCE and modified electrodes.

Electrode	i_a (μA)	i_c (μA)	E_a (V)	E_c (V)	ΔE (V)
GCE	8.75	-8.27	0.40	0.13	0.27
Nano-Au/GCE	8.62	-9.67	0.37	0.15	0.22
Nano-Au/CTAB/GCE	11.99	-10.31	0.41	0.13	0.28
Nano-Au/tween 80/GCE	12.96	-12.26	0.36	0.17	0.19
Nano-Au/SDBS/GCE	15.35	-13.27	0.29	0.19	0.10

Table 3. Comparable methods for determination of catechol

Method	Analyte	Linear working range	LOD	References
GCE	Catechol	3–400 μM	3 μM	[30]
(CMWNTs $NHCH_2CH_2NH)_6$/GCE	Catechol	5–80 μM	1.0 μM	[37]
MWCNT-PMG/GCE	Catechol	30–1190 μM	5.8 μM	[38]
Titrimetric	Catechol	20-1000 μg	20 μg	[39]
Spectrophotometric	Catechol	5-30 μg	5 μg	[39]
Polarographic	Catechol	1-1000 μg	1 μg	[39]
$[(CoTPRu_4)_n^{8+}$-GCE]/$AuNP^{n-}$	Catechol	21-1357 μM	1.4 μM	[40]
nano-Au/CTAB/GCE	Catechol	5-44 μM	3.43 μM	This work
		48-1039 μM	64.06	
nano-Au/Tween 80/GCE	Catechol	3-16 μM	1.56 μM	This work
		39.8-909.09 μM	64.2	
nano-Au/SDBS/GCE	Catechol	3-51.7 μM	7.32 μM	This work
		55.7-1666.7 μM	89.8	

Co; complex, TPyP; 5,10,15,20-tetrapyridilphorphyrin, dppb; 1,4-bis(diphenylphosphino)butane, gold nanoparticles; ($AuNPs^{n-}$)

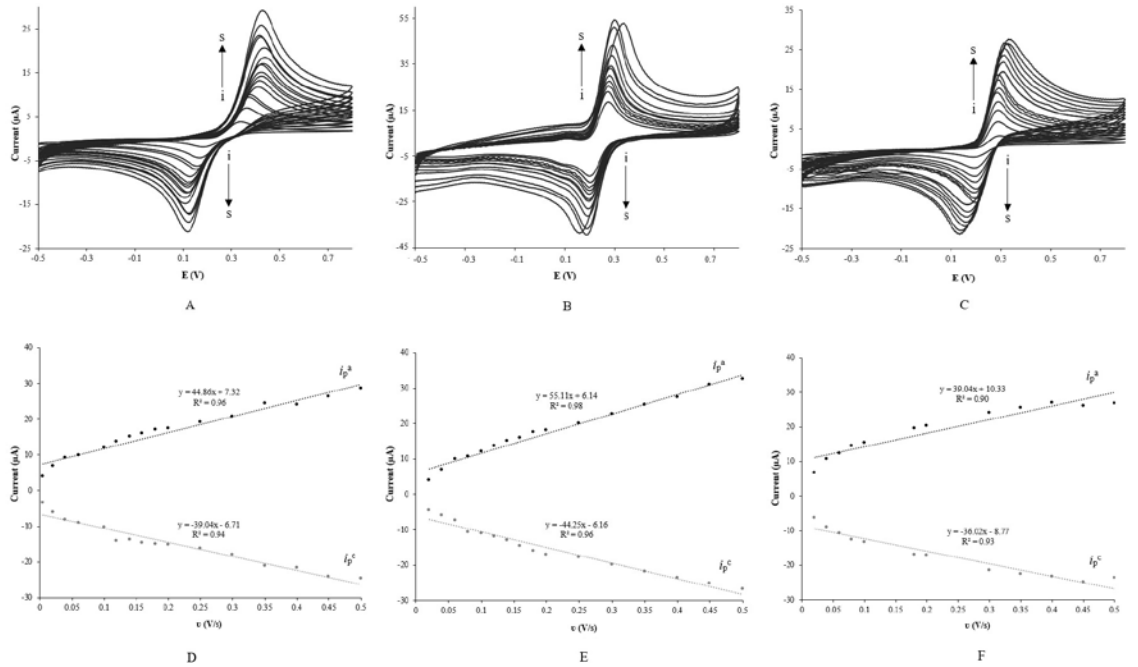

Fig. 4. CV voltammograms of (A) nano-Au/CTAB/GCE, (B) nano-Au/Tween 80/GCE, (C) nano-Au/ SDBS/GCE in PB (0.1 M, pH 6.0) containing 1.0 mM catechol at different scan rates. Scan rates from (e) to (i) are 20, 40, 60, 100, 150, 200, 250, 300, 350, 400, 450, 500 mV/s, respectively. Effect of scan rate on anodic and cathodic currents of (D) nano-Au/CTAB/GCE, (E) nano-Au/Tween 80/GCE, (F) nano-Au/ SDBS/GCE. Electrode area: 1.5 cm^2; scan rate: 100 mV/s

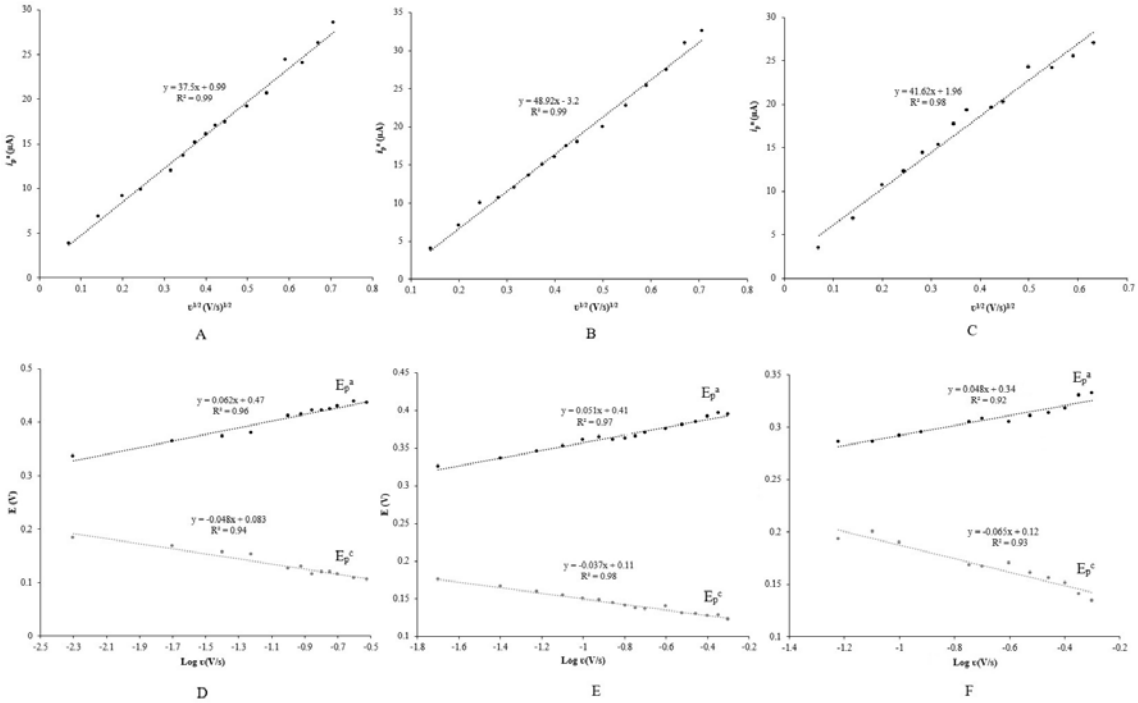

Fig. 5. Variation of anodic peak current (points) as a function of $v^{½}$ for (A) nano-Au/CTAB/GCE, (B) nano-Au/Tween 80/GCE, (C) nano-Au/ SDBS/GCE. Dependence of peak potentials versus scan rate in logarithmic scale for (D) nano-Au/CTAB/GCE, (E) nano-Au/ Tween 80/GCE, (F) nano-Au/ SDBS/GCE.

anodic and cathodic potentials (E_p^a - E_p^c) therefore it has the highest catalytic ability for catechol oxidation and reduction.

Effect of scan rate

Fig. 4 A,B,C shows the CVs of 1.0 mM catechol in PB solution (0.1 M) at different scan rates for the modified electrodes. The peak currents were observed to increase with increasing the scan rate (Fig. 4 D,E,F). According to Fig. 5 A,B,C, a linear relationship is found between the peak current and the square root of scan rate for modified electrodes. In the study of scan rates effect, we can distinguish the adsorption or diffusion control of analyte redox reaction. When the changing of currents versus different scan rates is linear, the mechanism of redox reaction is adsorption. While, when the currents have changed versus the square of scan rates, the mechanism of redox reaction is diffusion control. According to Fig. 4 and Fig. 5, the redox reaction of catechol for three modified electrodes is diffusion control [33]. Fig. 5 D,E,F displays the relationship between the anodic and cathodic potentials and the logarithm of scan rate (log υ) for modified electrodes in PB solution (0.1 M, pH 6) containing 1.0 mM of catechol. E_p^a has changed linearly versus log υ with a linear regression equation of $E_p^a = 0.062 \log \upsilon + 0.47$; $R^2 = 0.96$, $E_p^a = 0.036 \log \upsilon + 0.31$; $R^2 = 0.97$, $E_p^a = 0.018 \log \upsilon + 0.47$; $R^2 = 0.93$ in the range from 10 to 500 mV/s. For a redox monolayer modified electrode, the peak potentials can be represented by Laviron [34] (1) and (2):

$$E_p^a = E^{0\prime} - \frac{2.3RT}{(1-\alpha)nF}\log\frac{(1-\alpha)Fn\upsilon}{RTk} \quad (1)$$

$$\log k_s = \alpha\log(1-\alpha) + (1+\alpha)\log\alpha - \log\frac{RT}{nF\upsilon} - \frac{\alpha(1-\alpha)Fn\Delta E_p}{2.3RT} \quad (2)$$

Where α is the electron transfer coefficient, n is the number of electrons, R, T, F and k are gas, temperature, Faraday constant, and heterogeneous electron transfer rate constant, respectively. According to the slope of anodic process, α and n can be calculated. Given $0.3 < \alpha < 0.7$ in general [35], it could be concluded that n is equal to 2 and α is equal to 0.53, 0.42 and 0.39 for nano-Au/CTAB/GCE, nano-Au/Tween 80/GCE and nano-Au/SDBS/GCE, respectively. So, the redox reaction between electrodes and catechol is 2 electron transfer processes. Also, k could be estimated to be 0.015, 0.068, 0.55 s^{-1} for nano-Au/CTAB/GCE, nano-Au/Tween 80/GCE, and nano-Au/SDBS/GCE, respectively. According to these results, nano-Au/SDBS/GCE has the maximum heterogeneous electron transfer rate constant for catechol redox reaction. It can be related to the peak separations (ΔE_p) that are 0.286 V for nano-Au/CTAB/GCE, 0.211 V for nano-Au/Tween 80/GCE and 0.102 V for nano-Au/SDBS/GCE. Also, ΔE_p for nano-Au/SDBS/GCE is the smallest, possessing the maximum heterogeneous electron transfer rate constant. Moreover, it can be concluded that the reaction onto the surface of nano-Au/SDBS/GCE is the most reversible one.

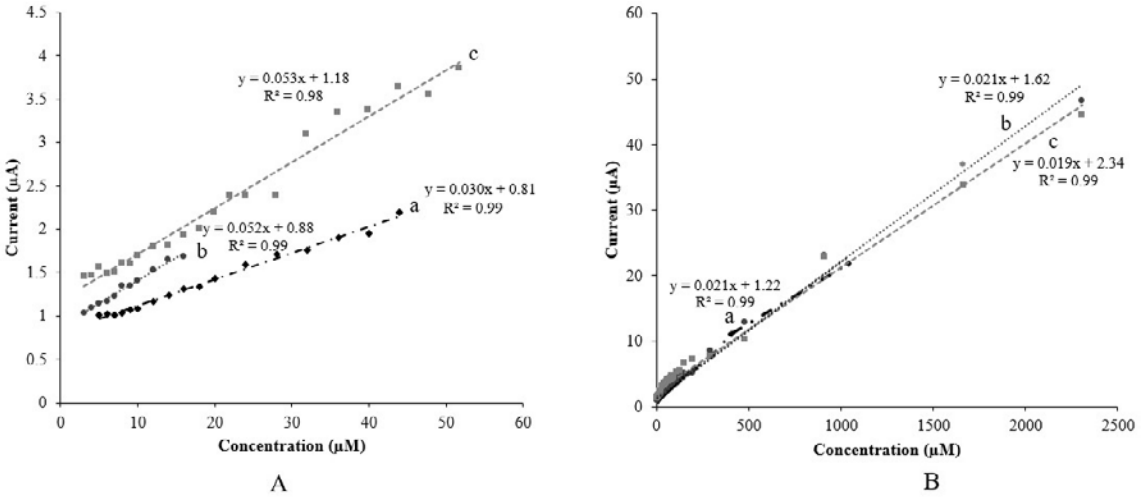

Fig. 6. Catechol calibration curves for (A) the first linear range and (B) the second linear range of nano-Au/CTAB/GCE (a), nano-Au/Tween 80/GCE (b), nano-Au/ SDBS/GCE (c).

Calibration curve and detection limit

To initially establish a linear range, sensitivity and detection limits, we commonly rely on the external standard method. A common misconception is that limit of detection which is the smallest concentration that can be measured. Instead, it is the concentration at which we can decide whether an element is present or not, that is, the point where we can just distinguish a signal from the background. LSV was used for direct determination of catechol. Catechol showed a well-defined anodic peak using the following conditions: electrode as a working electrode, LSV amplitude in PB (0.1 M, pH 6). Two linear ranges were obtained for each modified electrodes including 5-44 and 48-1039 µM (Fig. 6 A,B (curve a)) with correlation coefficients of 0.99, 0.99 for nano-Au/CTAB/GCE, 3-16 and 39.8-909.09 µM (Fig. 6 A,B (curve b)) with correlation coefficients of 0.99, 0.99 for nano-Au/Tween 80/GCE and 3-51.7 and 55.7-1666.7 µM (Fig. 6 A,B (curve c)) with correlation coefficients of 0.99, 0.98 for nano-Au/SDBS/GCE. The first and second linear ranges are widest for nano-Au/Tween 80/GCE. The LODs were calculated based on 3S/m to be 3.43 and 64.06 µM for nano-Au/CTAB/GCE, 1.56 and 64.2 µM for nano-Au/Tween 80/GCE and 7.32 and 89.8 µM for nano-Au/SDBS/GCE. Here, m is the slope of the first linear dynamic range of the calibration curve, and the value of S is the standard deviation of low concentration with a signal-to-noise ratio (S/N) of 3. Results of LOD calculation show nano-Au/Tween 80/GCE has the lowest LOD for the first linear range and nano-Au/CTAB/GCE has the lowest LOD for the second linear range. In Table 4, some common techniques are shown for catechol detection. Also, linear ranges and LODs are compared for modified electrodes of this study with other modified electrodes [29,36,37] and other techniques [38]. It is clear that linear ranges of nano-Au/surfactants/GCEs are wider than other modified electrodes [29,36,38] and the LOD of nano-Au/Tween 80/GCE is lower than values presented in literature [29,37].

CONCLUSIONS

A convenient and sensitive electrochemical method for determination of catechol was successfully demonstrated with the use of an Au/surfactant composite NPs modified GCEs. Au and three surfactants (CTAB, Tween 80, SDBS) were used to modify electrodes. This method is easier and more controllable than the common electrode modification techniques, such as drop and spinning coating. The electrochemical behavior of catechol on this modified electrode was thoroughly investigated. Nano- Au/SDBS/GCE has the maximum redox currents and *k* and the lowest cathodic and anodic peak potential deference. The results indicated that the modified electrodes exhibit good linear ranges and low detection limits to determine trace catechol in solution samples. The first and second linear ranges for nano-Au/Tween 80/GCE are widest. Results of LOD calculation show nano-Au/Tween 80/GCE has the lowest LOD for the first linear range and nano-Au/CTAB/GCE has the lowest LOD for the second linear range. Thus, the nano-Au/surfactant/GCEs show promising application for catechol detection in environmental monitoring.

CONFLICT OF INTEREST

The authors declare that there is no conflict of interests regarding the publication of this manuscript.

REFERENCES

1. C. Wang, Y. Feng, P. Gao, N. Ren and B.-L. Li, Sci. Total Environ., 431, 366 (2012).
2. M. Nazari, S. Kashanian, and R. Rafipour, Spectrochim. Acta Mol. Biomol. Spectrosc., 145, 130 (2015).
3. H. Chen, J. Yao, F. Wang, Y. Zhou, K. Chen, R. Zhuang, M.M.F. Choi and G. Zaray, Sci. Total Environ., 408, 1043 (2010).
4. N. Negash, H. Alemu, and M. Tessema, ISRN anal. chem., 2014 (2014).
5. M. Nazari, S. Kashanian, P. Moradipour, N. Maleki, J. Electroanal. Chem., 812, 122 (2018).
6. D. Talarico, F. Arduini, A. Constantino, M. Del Carlo, D. Compagnone, D. Moscone and G. Palleschi, Electrochem. commun., 60, 78 (2015).
7. X.-H. Zhou, L.-H. Liu, X. Bai and H.-C. Shi, Sens. Actuators B Chem., 181, 661 (2013).
8. N. Maleki, S. Kashanian, E. Maleki, M. Nazari, Biochem. Eng. J., 128, 1 (2017).
9. F.A. Gorla, E.H. Duarte, E.R. Sartori and C.R.T. Tarley, Microchem. J., 124, 65 (2016).
10. F. Maya, J.M. Estela and V. Cerdà, Talanta, 81, 1 (2010).
11. I. Cesarino, F.C. Moraes, T.C.R. Ferreira, M.R.V. Lanza and S.A.S. Machado, J. Electroanal. Chem., 672, 34 (2012).
12. J. Dobes, J. Sochor, P. Babula, J. Kynicky, J. Hubalek, B. Klejdus and R. Kizek, Int. J. Electrochem. Sci., 8, 4520 (2013).
13. H. Liang, X-B Zhang, Y. Lv, L. Gong, R. Wang, X. Zhu, R. Yang, and W. Tan, Acc. Chem. Res., 47, 1891 (2014).
14. K. Golchin, J. Golchin, S. Ghaderi, N. Alidadiani, S. Eslamkhah, M. Eslamkhah, S. Davaran and A. Akbarzadeh, Artif. Cells Nanomed. Biotechnol., ;1–5. doi: 10.1080/21691401.2017.1305393 [Epub ahead of print] (2017).
15. C. Morasso, S. Picciolini, D. Schiumarini, D. Mehn, I. Ojea-

Jime´nez, G. Zanchetta, R. Vanna, M. Bedoni, D. Prosperi, F. Gramatica, J. Nanopart. Res., 17, 330 (2015).
16. H. Ma, B. Yin, S. Wang, Y. Jiao, W. Pan, S. Huang, S. Chen and F. Meng, ChemPhysChem, 5, 68 (2004).
17. M.N. Khan, T.A. Khan, S.A. Al-Thabaiti and Z. Khan, Spectrochim. Acta Mol. Biomol. Spectrosc., 149, 889 (2015).
18. M.S. Bakshi, P. Sharma and T. S. Banipal, Mater. Lett., 61, 5004 (2007).
19. E.H. Duarte, L.T. Kubota and C.R.T. Tarley, Electroanalysis, 24, 2291 (2012).
20. W. Huang, C. Yang, W. Qu and S. Zhang, Russ. J. Electrochem., 44, 946 (2008).
21. F.F. Hudari, E.H. Duarte, A.C. Pereira, L.H. Dall'Antonia, L.T. Kubota and C.R.T. Tarley, J. Electroanal. Chem., 696, 52 (2013).
22. R. Jain, R. Mishra and A. Dwivedi, Colloids Surf., A, 337, 74 (2009).
23. B.J. Sanghavi and A.K. Srivastava, Electrochim. Acta, 55, 8638 (2010).
24. A. Levent, A. Altun, Y. Yardım and Z. Şentürk, Electrochim. Acta, 128, 54 (2014).
25. Y. Liu, Z. Zhang, L. Nie and S. Yao, Electrochim. Acta, 48, 2823 (2003).
26. Y. J. Yang, L. Guo, W. Zhang, J. Electroanal. Chem., 768, 102 (2016).
27. P. Patnaik, B. C. Tripathy, I. N. Bhattacharya, M. K. Ghosh, R. K. Paramguruc, Russ. J. Non-Ferr. Met., 57, 331 (2016).
28. J. Zhang, X-H Song, S. Ma, Xue Wang, Wen-chang Wang, Zhi-dong Chen, J. Electroanal. Chem., 795, 10 (2017).
29. C.F. Valezi, E.H. Duarte, G.R. Mansano, L.H. Dall'Antonia, C.R.T. Tarley and E.R. Sartori, Sens. Actuators B Chem., 205, 234 (2014).
30. J. Peng and Z.-N. Gao, Anal. Bioanal. Chem., 384, 1525 (2006).
31. Y. Zhao, Z. Wang, W. Zhang and Jiang, X., Nanoscale, 2, 2114 (2010).
32. Z. Wang, J. Yuan, M. Zhou, L. Niu and A. Ivaska, Appl. Surf. Sci., 254, 6289 (2008).
33. D. Song, J. Xia, F. Zhang, S. Bi, W. Xiang, Z. Wang, L. Xia, Y. Xia, Y. Li and L. Xia, Sens. Actuators B Chem., 206, 111 (2015).
34. D. Guzmán-Hernández, M. Ramírez-Silva, M. Palomar-Pardavé, S. Corona-Avendaño, A. Galano, A. Rojas-Hernández and M. Romero-Romo, Electroch. Acta, 59, 150 (2012).
35. E. Laviron, J. electroanal. chem. interfacial electrochem., 101, 19 (1979).
36. W. Sun, D. Wang, Z. Zhai, R. Gao and K. Jiao, J. Iran Chem. Soc., 6, 412 (2009).
37. S. Feng, Y. Zhang, Y. Zhong, Y. Li and S. Li, J. Electroanal. Chem., 733, 1 (2014).
38. Y. Umasankar, A.P. Periasamy and S.-M. Chen, Anal. biochem., 411, 71 (2011).
39. D. Amin and S.T. Sulaiman, Analyst, 109, 739 (1984).